

AD-A035 081

AIR FORCE MATERIALS LAB WRIGHT-PATTERSON AFB OHIO  
EFFECT OF STACKING SEQUENCE ON THE NOTCHED STRENGTH OF LAMINATE--ETC(U)  
NOV 76 J M WHITNEY, R Y KIM

F/G 11/4

UNCLASSIFIED

AFML-TR-76-177

'NL

1 OF 1  
AD-A  
035 081



**U.S. DEPARTMENT OF COMMERCE**  
**National Technical Information Service**

AD-A035 081

EFFECT OF STACKING SEQUENCE ON THE NOTCHED  
STRENGTH OF LAMINATED COMPOSITES

AIR FORCE MATERIALS LABORATORY  
WRIGHT-PATTERSON AIR FORCE BASE, OHIO

NOVEMBER 1976

ADA035081

AFML-TR-76-177

# EFFECT OF STACKING SEQUENCE ON THE NOTCHED STRENGTH OF LAMINATED COMPOSITES

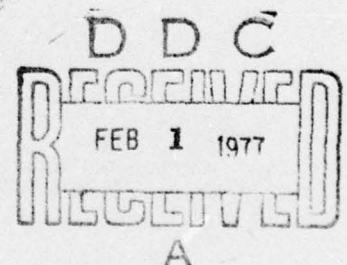
NOVEMBER 1976

TECHNICAL REPORT AFML-TR-76-177  
INTERIM REPORT FOR PERIOD 1 NOVEMBER 1975 - 1 MAY 1976

Approved for public release; distribution unlimited

REPRODUCED BY  
NATIONAL TECHNICAL  
INFORMATION SERVICE  
U. S. DEPARTMENT OF COMMERCE  
SPRINGFIELD, VA. 22161

AIR FORCE MATERIALS LABORATORY  
AIR FORCE WRIGHT AERONAUTICAL LABORATORIES  
AIR FORCE SYSTEMS COMMAND  
WRIGHT-PATTERSON AIR FORCE BASE, OHIO 45433

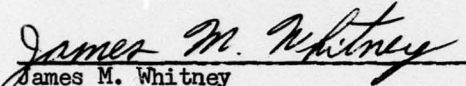


NOTICE

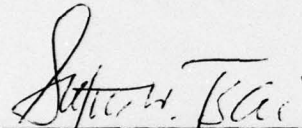
When Government drawings, specifications, or other data are used for any purpose other than in connection with a definitely related Government procurement operation, the United States Government thereby incurs no responsibility nor any obligation whatsoever; and the fact that the government may have formulated, furnished, or in any way supplied the said drawings, specifications, or other data, is not to be regarded by implication or otherwise as in any manner licensing the holder or any other person or corporation, or conveying any rights or permission to manufacture, use, or sell any patented invention that may in any way be related thereto.

This report has been reviewed by the Information Office (OI) and is releasable to the National Technical Information Service (NTIS). At NTIS, it will be available to the general public, including foreign nations.

This technical report has been reviewed and is approved for publication.

  
James M. Whitney  
Principal Investigator

FOR THE COMMANDER

  
Stephen W. Tsai, Chief  
Mechanics and Surface Interactions Branch  
Nonmetallic Materials Division

Copies of this report should not be returned unless return is required by security considerations, contractual obligations, or notice on a specific document.



## UNCLASSIFIED

SECURITY CLASSIFICATION OF THIS PAGE (When Data Entered)

REPORT DOCUMENTATION PAGE		READ INSTRUCTIONS BEFORE COMPLETING FORM
1. REPORT NUMBER AFML-TR-76-177	2. GOVT ACCESSION NO.	3. RECIPIENT'S CATALOG NUMBER
4. TITLE (and Subtitle) Effect of Stacking Sequence on The Notched Strength of Laminated Composites		5. TYPE OF REPORT & PERIOD COVERED Interim 1 November 75-1 May 76
		6. PERFORMING ORG. REPORT NUMBER
7. AUTHOR(s) J. M. Whitney R. Y. Kim		8. CONTRACT OR GRANT NUMBER(s) In-house
9. PERFORMING ORGANIZATION NAME AND ADDRESS Air Force Materials Laboratory (AFML/MBM) Air Force Wright Aeronautical Laboratories Wright-Patterson AFB, Ohio 45433		10. PROGRAM ELEMENT, PROJECT, TASK AREA & WORK UNIT NUMBERS 62102F/7340/734003/ 734003A8
11. CONTROLLING OFFICE NAME AND ADDRESS Air Force Materials Laboratory (AFML/MBM) Air Force Wright Aeronautical Laboratories Wright-Patterson AFB, Ohio 45433		12. REPORT DATE November 1976
14. MONITORING AGENCY NAME & ADDRESS (if different from Controlling Office)		13. NUMBER OF PAGES 31
		15. SECURITY CLASS. (of this report) Unclassified
15a. DECLASSIFICATION/DOWNGRADING SCHEDULE		
16. DISTRIBUTION STATEMENT (of this Report)  Approved for public release, distribution unlimited.		
17. DISTRIBUTION STATEMENT (of the abstract entered in Block 20, if different from Report)  Approved for public release, distribution unlimited.		
18. SUPPLEMENTARY NOTES		
19. KEY WORDS (Continue on reverse side if necessary and identify by block number) Fracture properties                      Fracture strength Composite materials                      Failure Stacking sequence effect                      Notch strength		
20. ABSTRACT (Continue on reverse side if necessary and identify by block number) The effect of laminate stacking sequence on the notched and unnotched tensile strength of quasi-isotropic graphite/epoxy laminates is investigated. Notch geometry includes circular holes and center cracks. Experimental data is presented for two different stacking sequences of quasi-isotropic graphite/epoxy laminates. One stacking sequence produces large interlaminar tensile stresses along straight free-edges of a tensile coupon, (continued over)		

DD FORM 1 JAN 73 1473

EDITION OF 1 NOV 65 IS OBSOLETE

UNCLASSIFIED

SECURITY CLASSIFICATION OF THIS PAGE (When Data Entered)

UNCLASSIFIED

SECURITY CLASSIFICATION OF THIS PAGE(When Data Entered)

<sup>2</sup>) +

20. (Abstract, continued)

while the second yields compression at the same free-edges. Three different notch sizes are used for the circular hole and center crack in conjunction with both stacking sequences. Each data point is represented by a minimum of fifteen replicates so that statistical distributions of notched and unnotched strengths can be obtained. The experimental data indicates that unnotched tensile strength is reduced by the presence of interlaminar tensile stresses at the straight free-edge, while notched strength appears to be independent of stacking sequence for notch sizes which produce tensile failure prior to delamination at the straight free-edge.

Experimental results are also compared against theoretical notch strengths obtained from the average stress criterion and the point stress criterion, two recently developed criteria for predicting notch strength of laminated composites.

UNCLASSIFIED

SECURITY CLASSIFICATION OF THIS PAGE(When Data Entered)

(a)

## FOREWORD

In this report, the effect of laminate stacking sequence on the tensile strength of notched and unnotched graphite/epoxy laminates is investigated.

The work reported here was performed in the Mechanics and Surface Interactions Branch, Nonmetallic Materials Division, Air Force Materials Laboratory, Wright-Patterson Air Force Base, Ohio. James M. Whitney, AFML/MBM, was the principal investigator. The authors wish to acknowledge J. Camping, R. Esterline, T. Richardson and C. Lovett of the University of Dayton Research Institute for the fabrication, preparation and testing of composite experimental specimens. This report was released by the authors, J. M. Whitney and R. Y. Kim in August 1976, and covers the time period of November 1975 to May 1976.

ADDITIONAL FOR	
NTS	White Section <input checked="" type="checkbox"/>
900	Buff Section <input type="checkbox"/>
UNCLASSIFIED	
CLASSIFICATION	
DISTRIBUTION/AVAILABILITY CODE	
Stat	AVAIL. UNCL. UNCL.
A	



## TABLE OF CONTENTS

SECTION		PAGE
I.	INTRODUCTION .....	1
II.	EXPERIMENTAL PROGRAM .....	2
III.	DATA REDUCTION .....	5
VI.	DISCUSSION AND CONCLUSIONS.....	8
	REFERENCES.....	10

**Preceding page blank**



# LIST OF ILLUSTRATIONS

FIGURE		PAGE
1	Free-body diagram for determining interlaminar stress transfer mechanisms .....	14
2	Approximate distribution of interlaminar normal stress at laminate mid-plane ( $z = 0$ ) .....	15
3	Distribution of interlaminar normal stress through laminate thickness at the free-edges ( $y = \pm W/2$ ) of a tensile coupon.....	16
4	Geometry of circular hole and center cracked tensile specimen.....	17
5	Comparison of predicted and experimental failure stresses for circular holes.....	18
6	Comparison of predicted and experimental failure stresses for center cracks .....	19
7	Typical longitudinal and axial stress-strain response of unnotched laminates.....	20
8	Typical data fit to linearized Weibull distribution.....	21
9	Comparison of Weibull distributions for unnotched laminates and laminates containing a center crack, $(\pm 45, 0, 90)_s$ stacking sequence.....	22
10	Comparison of Weibull distributions for laminates containing a circular hole, $(\pm 45, 0, 90)_s$ stacking sequence.....	23
11	Comparison of Weibull distribution for unnotched laminates and laminates containing a center crack, $(90, 0, \pm 45)_s$ stacking sequence.....	24
12	Comparison of Weibull distributions for laminates containing a circular hole, $(90, 0, \pm 45)_s$ stacking sequence.....	25

## LIST OF TABLES

TABLE		PAGE
1	ELASTIC PROPERTIES T300/934 .....	11
2	TEST PROGRAM .....	12
3	EXPERIMENTAL RESULTS .....	13

## SECTION I

### INTRODUCTION

Delamination along straight free-edges of composite laminates in the presence of an in-plane uniaxial load has been previously observed, for example, see References 1 and 2 . Such a phenomenon is associated with interlaminar tensile stresses generated along straight free-edges. The nature and determination of interlaminar stresses at free-edges has received detailed discussion in previous publications [3, 4, 5, 6]. The laminate stacking sequence will determine whether an interlaminar normal stress will produce tension or compression at the straight free-edge of a tensile coupon. Thus, it is possible that the in-plane tensile strength of laminated composites could be influenced by ply stacking sequence. Since notches present free-edges of a different nature than those of a straight edge in an unnotched tensile coupon, they are also of interest.

In the present paper, the effect of stacking sequence on the notched and unnotched tensile strength of quasi-isotropic graphite/epoxy laminates is investigated experimentally. Notches consist of circular holes and center cracks. Results are presented for two stacking sequences, one which produces large interlaminar tensile stresses along straight free-edges of a coupon and a second which produces interlaminar compression along the same free-edges.

## SECTION II

### EXPERIMENTAL PROGRAM

The material system chosen for this investigation is Fiberite's T300/934 graphite/epoxy system referred to by Fiberite as the 1034 pre-preg system. Two quasi-isotropic laminate stacking sequences were used,  $(\pm 45, 0, 90)_s$  and  $(90, 0, \pm 45)_s$ . The laminate with the  $\pm 45$ -degree plies on the outside produce interlaminar tension at the straight edge of a tensile coupon as illustrated in Figure 1. In particular, the free-body diagram indicates clockwise bending moments produced by the interlaminar normal stress  $\sigma_z$  at the free-edge, which produces a tensile stress. The largest value of  $\sigma_z$  occurs along the laminate centerline. The calculations used to establish Figure 1 are based on the following assumptions: (1) plane stress laminated plate theory [7,8,9] is recovered at the central plane of the laminate  $y=0$ , provided the width,  $W$ , is considerably larger than the thickness,  $h$  ( $W/h \gg 2$ ); (2) the force and moment resultants which are statically equivalent to the interlaminar stresses along planes  $z = \text{constant}$  can be determined from simple equilibrium of forces and moments; (3) the interlaminar stresses are confined to a boundary region adjacent to the free-edges  $y = \pm W/2$  which is approximately equal to the laminate thickness. This procedure was first proposed by Pagano and Pipes [4]. The following ply elastic properties were used to obtain the results in Figure 1:

$$\begin{aligned} E_L &= 21 \times 10^6 \text{ psi}, \quad E_T = 1.6 \times 10^6 \text{ psi} \\ G_{LT} &= 0.7 \times 10^6 \text{ psi}, \quad \nu_{LT} = 0.3 \end{aligned} \tag{1}$$

where  $L$  is the fiber direction,  $T$  the transverse direction, and  $\nu_{LT}$  is the Poisson ratio determined by measuring the transverse strain in a uniaxial tensile test parallel to the fibers.

Using the moments produced by  $\sigma_z$ , as shown in Figure 1, the distribution of  $\sigma_z$  across the width of the laminate on any plane  $z=\text{constant}$  can be



estimated from the procedure developed by Pagano and Pipes [2]. Results of this estimate are shown in Figure 2 at  $z = 0$ . Now noting that the stresses in the tensile coupon are independent of  $x$ , the distribution of  $\sigma_z$  through the laminate thickness can be determined from the equilibrium equation of elasticity theory

$$\tau_{yz,y} + \sigma_{z,z} = 0 \quad (2)$$

From the free-body diagram in Figure 1 it can be seen that  $\tau_{yz}$  is linear within the  $i$ th ply, that is

$$\tau_{yz}^i = a_0^i + z a_1^i(y) \quad (3)$$

where  $a_0^i$  is a constant determined from continuity of  $\tau_{yz}^i$  at ply interfaces and  $a_1$  is a function of  $y$  only. Substituting Eq.(3) into Eq. (2) yields

$$\sigma_z^i = \int_{-h/2}^z (a_0^i + z a_1^i) dz \quad (4)$$

Since the integration is performed continuously from the bottom of the laminate, continuity of  $\sigma_z$  is assured at the layer interfaces. The distribution of  $\sigma_z$  through the laminate thickness is shown in Figure 3 for both laminate stacking sequences. Results for the  $(90, 0, \pm 45)_s$  laminate was obtained by following the same procedure as in Figures 1 and 2 in conjunction with Eq. 4.

It should be noted that the interlaminar stress distributions around holes and cracks are very complex with the interlaminar normal stress at each interface oscillating from tension to compression along the free-edges [10]. Thus, the effect of delamination around notches may be less severe than along the straight edges of a notched or unnotched coupon when  $\sigma_z$  produces tension along the entire free-edge.

The experimentally determined elastic properties of the two stacking sequences are shown in Table 1. As anticipated, the elastic constants are

relatively independent of stacking sequence effects. Dimensions of the test specimens are displayed in Figure 4. The effect of notch shape and size in conjunction with stacking sequence are examined by considering both circular holes and sharp-tipped center cracks of sizes 0.1, 0.3, and 0.6 in. (hole diameter or crack length).

A total of 296 test specimens were run, as shown in Table 2. Each data point is represented by a minimum of 15 replicate tests (see Table 2). This number of replicates is considered to be an absolute minimum number necessary for determining a statistical distribution of notched and unnotched strengths.

All specimens were cut from flat plates laid up and cured in an autoclave using the pre-preg supplier's recommended cure cycle. None of the panels received post-cure. Fiber volume fractions were determined to be approximately 65 percent. Unnotched specimens and notched specimens were cut from various panels in a rather random fashion. Thus, each data point is represented by replicates taken from a number of different panels.

Each notched specimen was a straight-sided tension specimen (see Figure 4) with either a centrally located drilled hole of the proper size or a central crack formed by drilling a 0.01 in.-diameter pilot hole and then using a 0.005 in.-diameter diamond wire to complete the crack. No attempt was made to make specimens with identical discontinuity length-to-width ratios (i.e.  $2R/W$  or  $2C/W$ ). In particular, although the gage length was constant,  $2R/W$  or  $2C/W$  was nominally 0.1, 0.2, and 0.3 for 0.1, 0.3, and 0.6 in. notch sizes, respectively.

All specimens were ramp loaded to failure at a rate of 20 lb/sec. in a closed-loop MTS machine. Acoustic emission was recorded for most specimens.

### SECTION III

#### DATA REDUCTION

The failure stress,  $\sigma_o$ , of unnotched tensile coupons was calculated from the failure load. In a similar manner, the failure stress of notched coupons,  $\sigma_N$ , was determined from their failure load. The notched values were adjusted by multiplying  $\sigma_N$  by isotropic finite width correction factors, as described in Reference 11, to obtain the notched, infinite width failure stress. Each set of data was fit to the Weibull distribution

$$P(\sigma_o > \sigma) = \exp \left[ -(\sigma/\hat{\sigma})^a \right] \quad (4)$$

where  $\sigma$  is the location parameter of the distribution, often referred to as the characteristic strength, and  $a$  is the shape parameter. Equation (4) was used in the following linearized form for purposes of fitting the data.

$$\frac{1}{a} \left[ \ln(-\ln P) \right] + \ln \hat{\sigma} = \ln \sigma \quad (5)$$

Average values, coefficient of variation,  $\eta$ , shape parameter, characteristic strength, and goodness of fit parameter,  $r$ , are shown in Table 3 for each data set. The parameter  $r$ , is a measure of how well the data fits Equation 5. For a perfect fit  $r = 1$ . A pooled value of the shape parameter,  $a_p$ , is also shown in Table 3 for each stacking sequence. This number was obtained by normalizing each data set with respect to its characteristic strength and pooling the resulting data to obtain a single value of the shape parameter. This procedure is based on the assumption that the shape parameter for notched and unnotched laminates of like material and ply orientations are the same, as discussed in References 11 and 12. The validity of this pooling procedure has been discussed by Lemon [13]. Thus,  $a_p$  is based on 147 specimens for the  $(\pm 45, 0, 90)_s$  laminate and on 149 specimens for the  $(90, 0, \pm 45)_s$  laminates.

Notched data was also compared to the point stress criterion and average stress criterion, which were previously developed in Reference 14 for predicting the strength of laminates under uniaxial load containing either a circular hole or center crack. Both criteria involve two parameters, unnotched tensile strength and a characteristic dimension adjacent to the



discontinuity,  $d_o$  for the point stress criterion and  $a_o$  for the average stress criterion. For a circular hole of radius  $R$  in a quasi-isotropic laminate

$$\frac{\sigma_N}{\sigma_o} = \frac{2}{2 + \xi_1^2 + 3\xi_1^4} \quad (6)$$

for the point stress criterion, and

$$\frac{\sigma_N}{\sigma_o} = \frac{2(1 - \xi_2)}{2 - \xi_2^2 - \xi_2^4} \quad (7)$$

for the average stress criterion where

$$\xi_1 = \frac{R}{R + d_o} \quad (8)$$

and

$$\xi_2 = \frac{R}{R + a_o} \quad (9)$$

For a center crack of length  $2c$  in an isotropic or orthotropic laminate,

$$\frac{\sigma_N}{\sigma_o} = \sqrt{1 - \xi_3^2} \quad (10)$$

for the point stress criterion and

$$\frac{\sigma_N}{\sigma_o} = \sqrt{\frac{1 - \xi_4}{1 + \xi_4}} \quad (11)$$

for the average stress criterion where

$$\xi_3 = \frac{C}{C + d_o} \quad (12)$$

and

$$\xi_4 = \frac{C}{C + a_o} \quad (13)$$

Results are shown in Figures 5 and 6 for the circular hole and center crack. Values of  $d_o = 0.04$  in. and  $a_o = 0.15$  in. were chosen, as these numbers had



been previously shown to give reasonable results for a variety of notched laminates  $[11]$ . Thus, no attempt was made to obtain a "best fit value" for  $d_o$  and  $a_o$ . Experimental data shown in Figures 5 and 6 are based on characteristic strengths shown in Table 3.

## SECTION IV

### DISCUSSION AND CONCLUSIONS

A cursory examination of Table 3 reveals that the unnotched tensile strength was effected by stacking sequence, while the notched strength shows very little sensitivity to stacking sequence. The reduction in unnotched tensile strength of the  $(\pm 45, 0, 90)_s$  laminates is attributed to gross delamination which occurred between 45 and 50 ksi axial tensile stress. In addition to being visible physically, delamination could be determined from the response of both longitudinal and transverse strain gages as shown in Figure 7. A sharp increase in total acoustic emission counts was also observed at the onset of delamination. The acoustic emission count as a function of axial strain is also illustrated in Figure 7 for a  $(\pm 45, 0, 90)_s$  laminate. Linear elastic response to failure for both longitudinal and transverse strain is observed for  $(90, 0, \pm 45)_s$  laminates, as seen in Figure 7. It should be noted from Figure 3 that the interlaminar normal stress,  $\sigma_z$ , at the free-edge is tension throughout the laminate thickness for the  $(\pm 45, 0, 90)_s$  stacking sequence, and in compression throughout the laminate thickness for the  $(90, 0, \pm 45)_s$  stacking sequence. The stress distributions in Figure 3 indicate that an axial tensile stress of 45-50 ksi corresponds to an estimated maximum value of  $\sigma_z$  of 17.4 -19.4 ksi.

In most cases for the notched specimens, tensile failure took place prior to delamination at the straight free-edge, preventing this failure mode from having any significant influence on notched strength. Since stacking sequence had little effect on notched strength, it is concluded that any delamination occurring along the free-boundary of the discontinuity either had little influence on ultimate strength or had the same effect on both stacking sequences. As pointed out earlier, interlaminar stress distributions on the boundary of through-the-thickness discontinuities are usually complex, yielding normal stresses which can oscillate from tension to compression along the free-edge.

As a point of academic interest, the ply properties of Eq. 1 in conjunction with lamination theory [7, 8, 9] yield  $E_{11} = 8.10 \times 10^6$  psi and  $\nu_{12} = 0.317$ . This compares favorably with the measured properties of Table 1.

Typical data points fit to Eq. 5 are illustrated in Figure 8. A comparison of Weibull distributions for unnotched data and notched data for  $(\pm 45, 0, 90)_s$  laminates is shown in Figures 9 and 10, and for  $(90, 0, \pm 45)_s$  laminates in Figures 11 and 12. It can be seen that the distributions for different sized circular holes and center cracks look very similar, while the unnotched distribution is broader with a longer tail, reflecting the lower value of  $a$  and correspondingly higher coefficient of variation. This data indicates that notched and unnotched tensile strength for the same laminate do not necessarily yield similar Weibull distributions. It has been previously postulated [11, 12, 15] that similar distributions should be obtained for notched and unnotched specimens of the same laminate.

Comparison between experiment and theory in Figures 5 and 6 show reasonably good agreement for both stacking sequences. It is possible that better agreement could be obtained from other choices of  $a_o$  and  $d_o$ .



# REFERENCES

1. J. M. Whitney and C. E. Browning, Journal of Composite Materials, Vol. 6, 1972, pp. 300-303.
2. N. J. Pagano and R. B. Pipes, International Journal of Mechanical Sciences, Vol. 15, 1973, pp. 679-688.
3. R. B. Pipes and N. J. Pagano, Journal of Composite Materials, Vol. 4, 1970, pp. 538-548.
4. N. J. Pagano and R. B. Pipes, Journal of Composite Materials, Vol. 5, 1971, pp. 50-57.
5. E. F. Rybicki, Journal of Composite Materials, Vol. 5, 1971, pp. 354-360.
6. N. J. Pagano, Journal of Composite Materials, Vol. 8, 1974, pp. 65-82.
7. Y. Stavsky, "Proceedings of the American Society of Civil Engineers", Journal of the Engineering Mechanics Division, Vol. 81, 1962, pp. 31-55.
8. J. E. Ashton and J. M. Whitney, Theory of Laminated Plates, Technomic Publishing Company, Stamford, Connecticut, 1970.
9. N. J. Pagano, Mechanics of Composite Materials, Edited by G. P. Sendeckyj, Volume 2 of Composite Materials Series, Edited by L. J. Broutman and R. H. Krock, Academic Press, New York, 1974, pp. 23-45.
10. E. F. Rybicki and A. T. Hopper, Analytical Investigation of Stress Concentrations Due to Holes in Fiber Reinforced Plastic Laminated Plates, 3-Dimensional Models, Air Force Technical Report AFML-TR-73-100, Air Force Materials Laboratory, June 1973.
11. R. J. Nuismer and J. M. Whitney, Fracture Mechanics of Composites, ASTM STP 593, American Society for Testing and Materials, 1975, pp. 117-142.
12. M. E. Waddoups and J. C. Halpin, Computers and Structures, Vol. 4, 1974, pp. 1-14.
13. R. V. Wolff and G. H. Lemon, Reliability Prediction for Composite Joints--Bonded and Bolted, Air Force Technical Report AFML-TR-74-197, March 1976.
14. J. M. Whitney and R. J. Nuismer, Journal of Composite Materials, Vol. 8, pp. 253-265.
15. J. M. Whitney, "Proceedings 12th Annual Meeting Society of Engineering Science", The University of Texas at Austin, 1975, pp. 173-182.



TABLE 1, ELASTIC PROPERTIES T300/934

ORIENTATION	$E_{11}$ (PSI)	$\nu_{12}$
$(\pm 45, 0, 90)_s$	* $7.68 \times 10^6$	* 0.30
$(90, 0, \pm 45)_s$	** $7.94 \times 10^6$	** 0.29

\* Based on an average of nine specimens

\*\* Based on an average of eight specimens

TABLE 2, TEST PROGRAM

TYPE	NOTCH SIZE			
	0	0.1"	0.3"	0.6"
Unnotched - 1*	31	---	---	---
Hole - 1	---	23	21	20
Crack - 1	---	18	19	15
Unnotched - 2**	32	---	---	---
Hole - 2	---	23	20	21
Crack - 2	---	19	18	16

\* 1 - Refers to  $(\pm 45, 0, 90)_s$

\*\* 2 - Refers to  $(90, 0, \pm 45)_s$

TABLE 3. EXPERIMENTAL RESULTS

	$(\pm 45, 0, 90)_s$						$(90, 0, \pm 45)_s$						$\frac{\hat{\sigma}(45)}{\hat{\sigma}(90)}$
	$\sigma_{avg}$ (psi)	$\eta(\%)$	$\hat{\sigma}$ (psi)	$\alpha$	r		$\sigma_{avg}$ (psi)	$\eta(\%)$	$\hat{\sigma}$ (psi)	$\alpha$	r		
Unnotched	65,434	7.2	67,613	15.6	0.97		72,398	7.8	74,941	14.7	.99		0.902
0.1" Hole	48,107	3.5	48,725	41.7	0.94		46,776	5.6	49,995	20.1	.95		0.975
0.3" Hole	39,618	3.6	40,239	30.1	0.92		39,573	4.2	40,340	27.2	.98		0.998
0.6" Hole	34,070	4.3	34,750	26.4	0.95		33,802	6.2	34,771	18.1	.96		0.999
0.1" Crack	47,044	4.3	47,971	26.6	0.98		47,219	6.5	48,657	17.0	.93		0.986
0.3" Crack	38,896	2.8	39,434	38.5	0.94		37,064	4.8	37,873	23.9	.98		1.041
0.6" Crack	32,211	5.5	33,057	19.6	0.97		31,106	7.0	32,119	15.6	.98		1.029
Pooled	----	*6.0	1.0006	21.4	0.98		----	*6.8	0.9995	18.0	1.00		---

\* Theoretical value based on pooled  $\alpha$



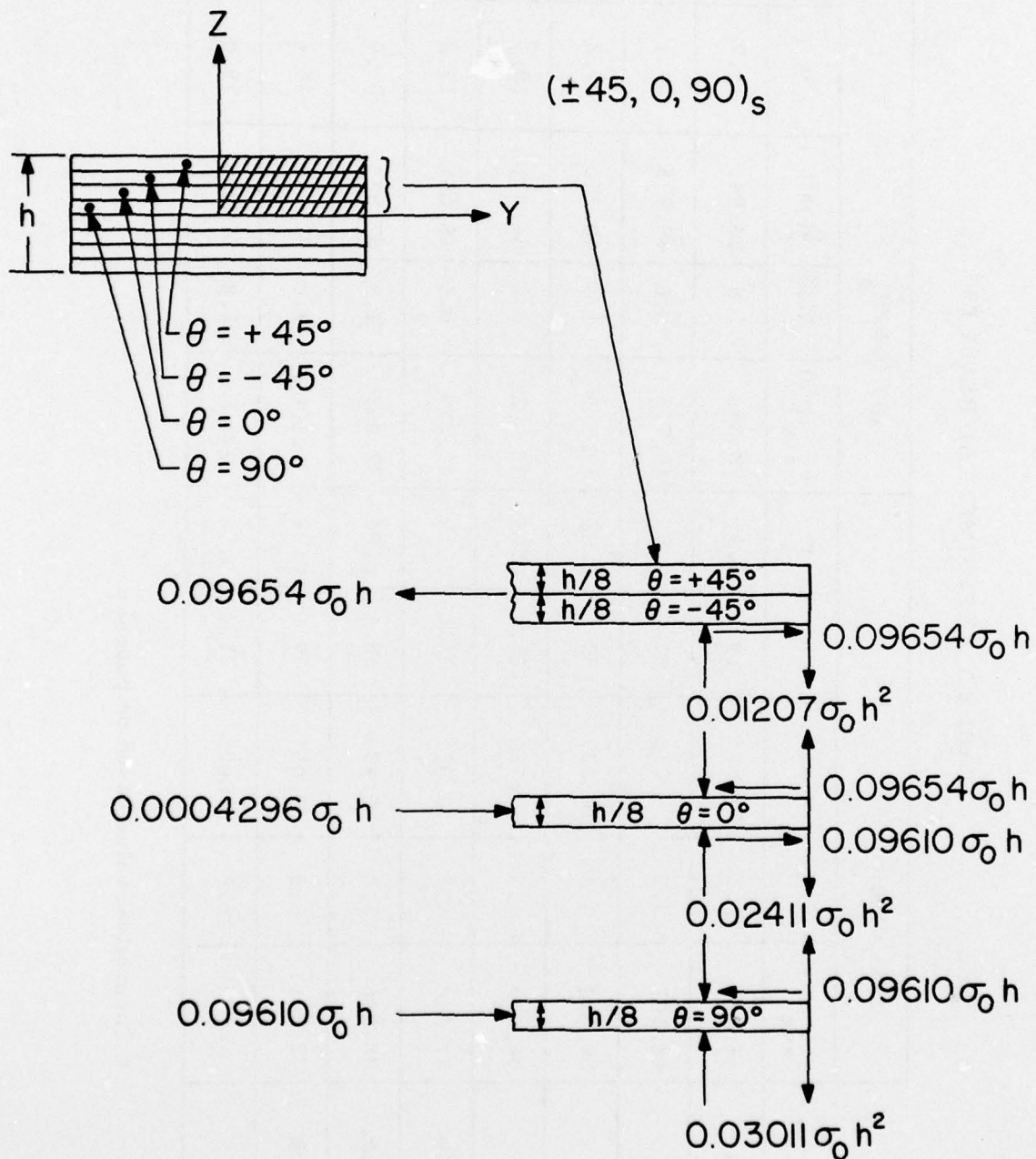


Figure 1. Free-body diagram for determining interlaminar stress transfer mechanisms.

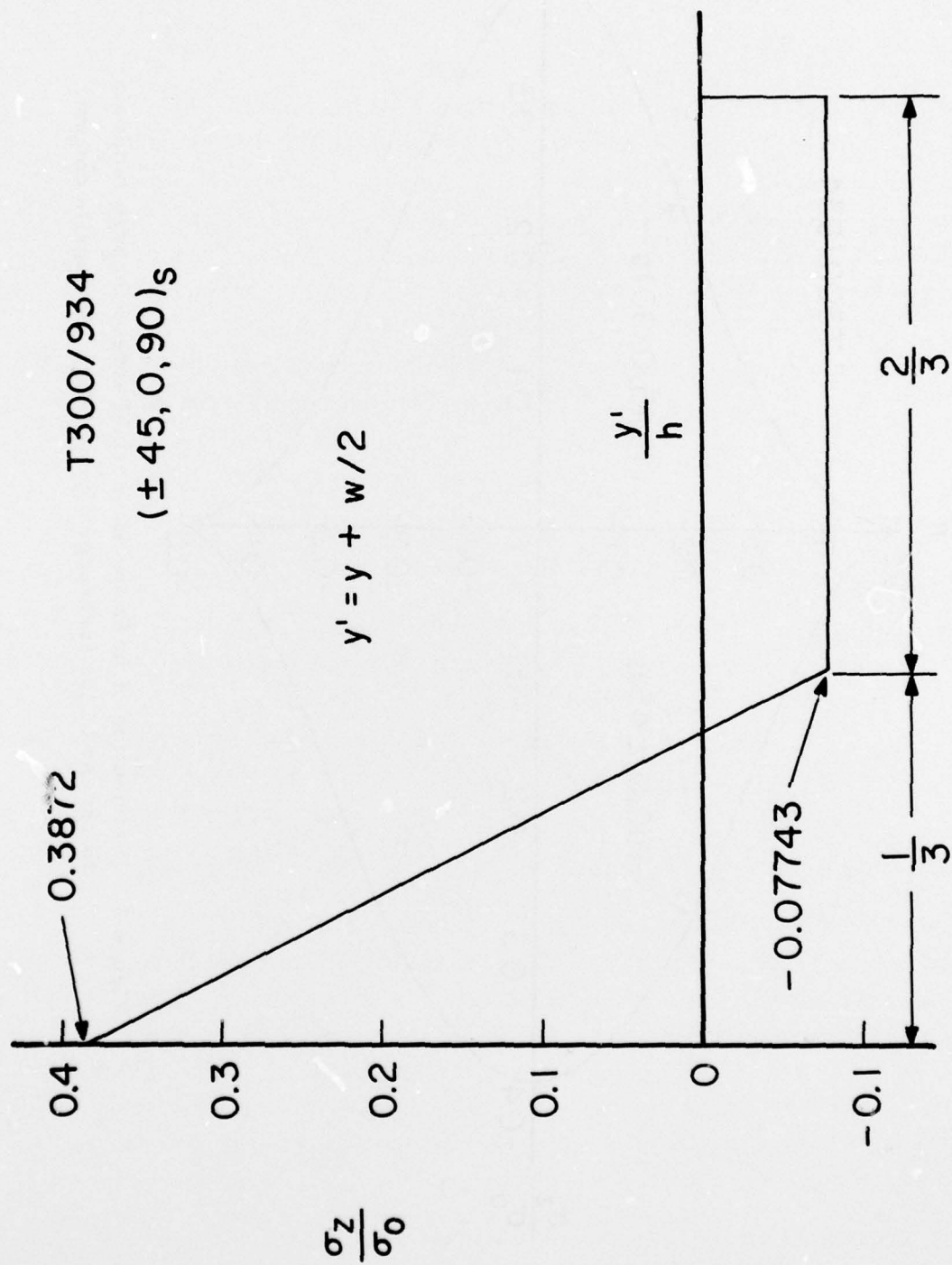


Figure 2. Approximate distribution of interlaminar normal stress at laminate mid-plane ( $z = 0$ ).

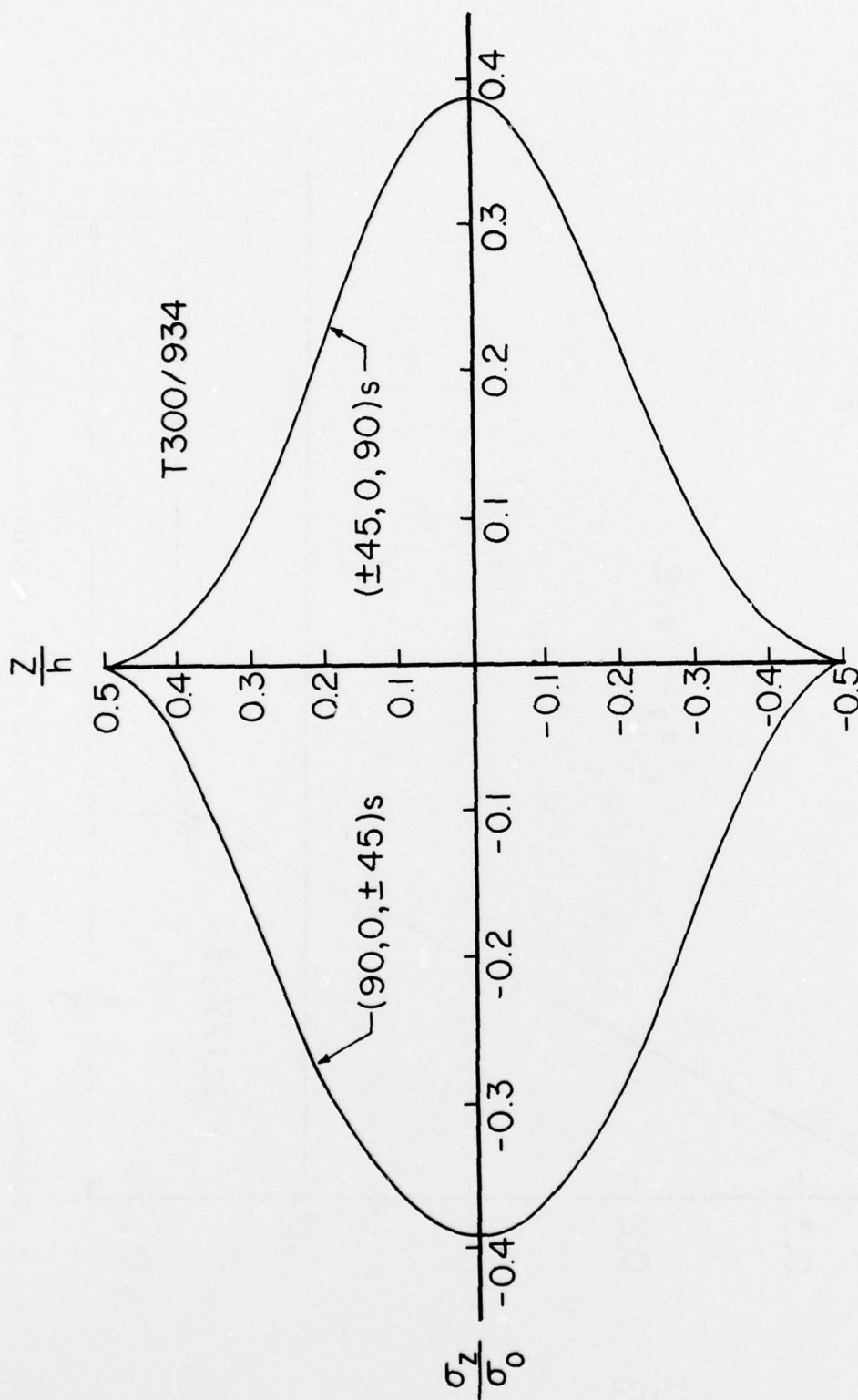
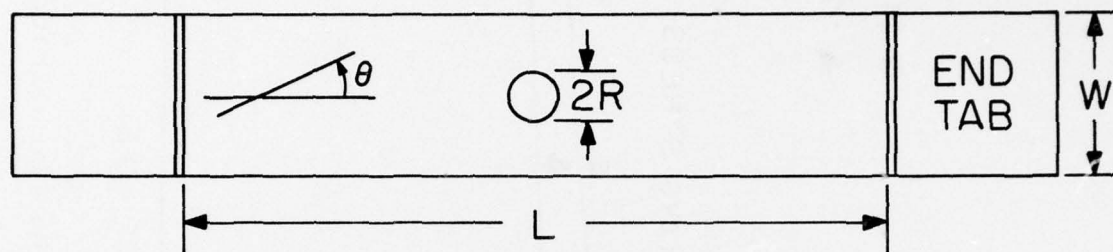
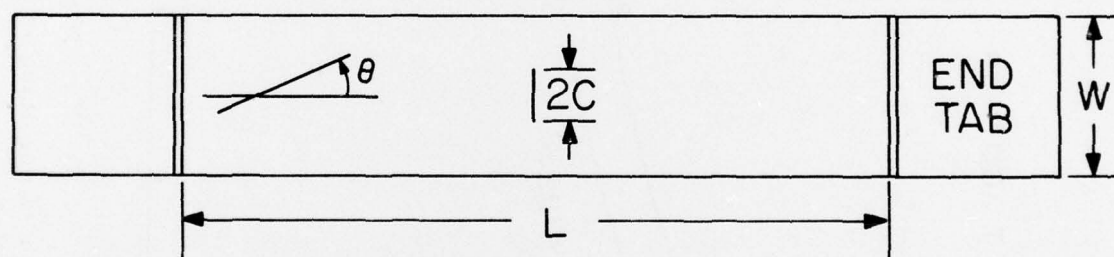


Figure 3. Distribution of interlaminar normal stress through laminate thickness at the free-edges ( $y = \pm W/2$ ) of a tensile coupon.





(a) HOLE



(b) CRACK

$$\frac{2R}{2C} = 0.1, 0.3, 0.6''$$

$$W = 1'', 1\frac{1}{2}'', 2''$$

$$L = 9''$$

Figure 4. Geometry of circular hole and center cracked tensile specimens.

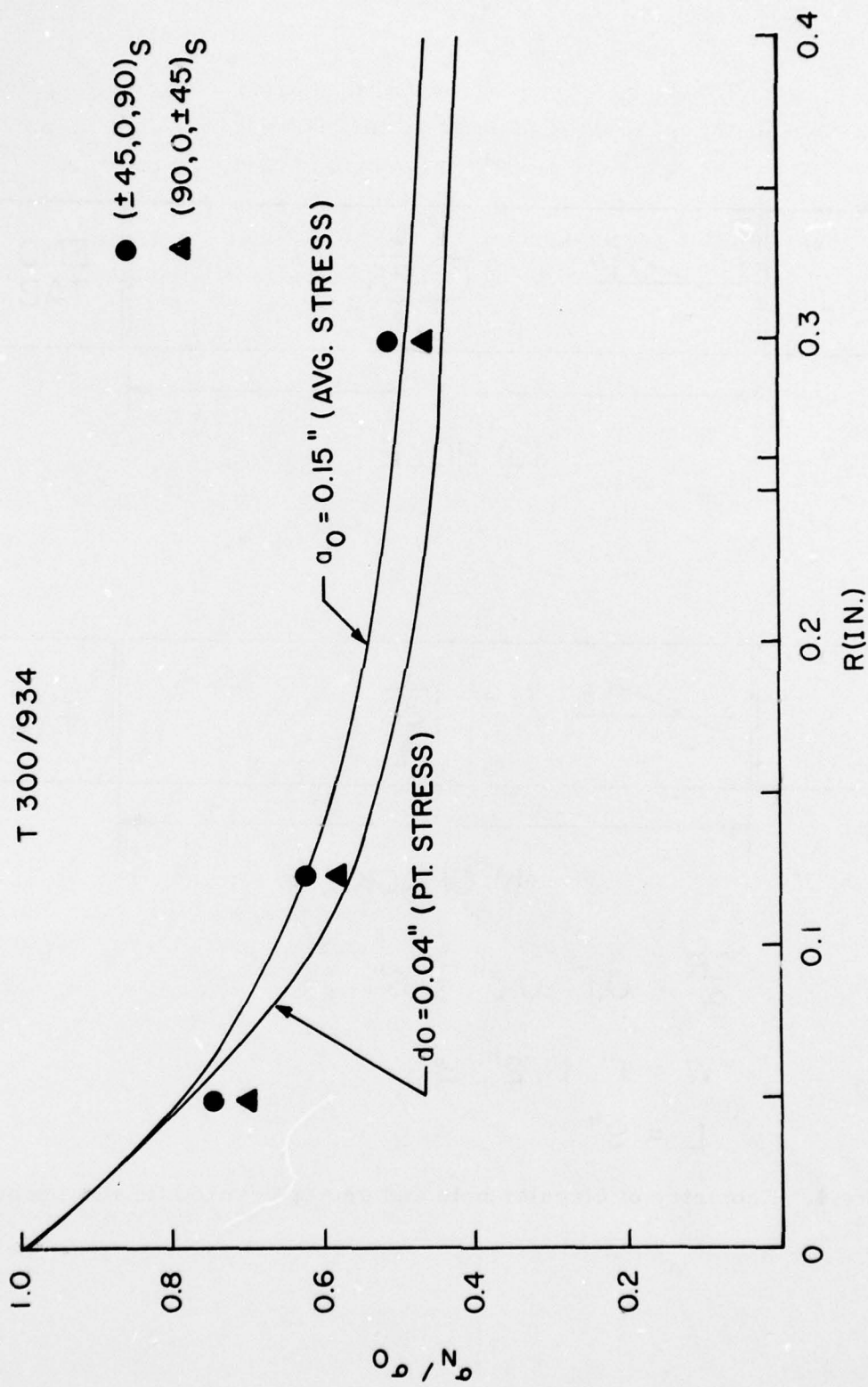


Figure 5. Comparison of predicted and experimental failure stresses for circular holes.

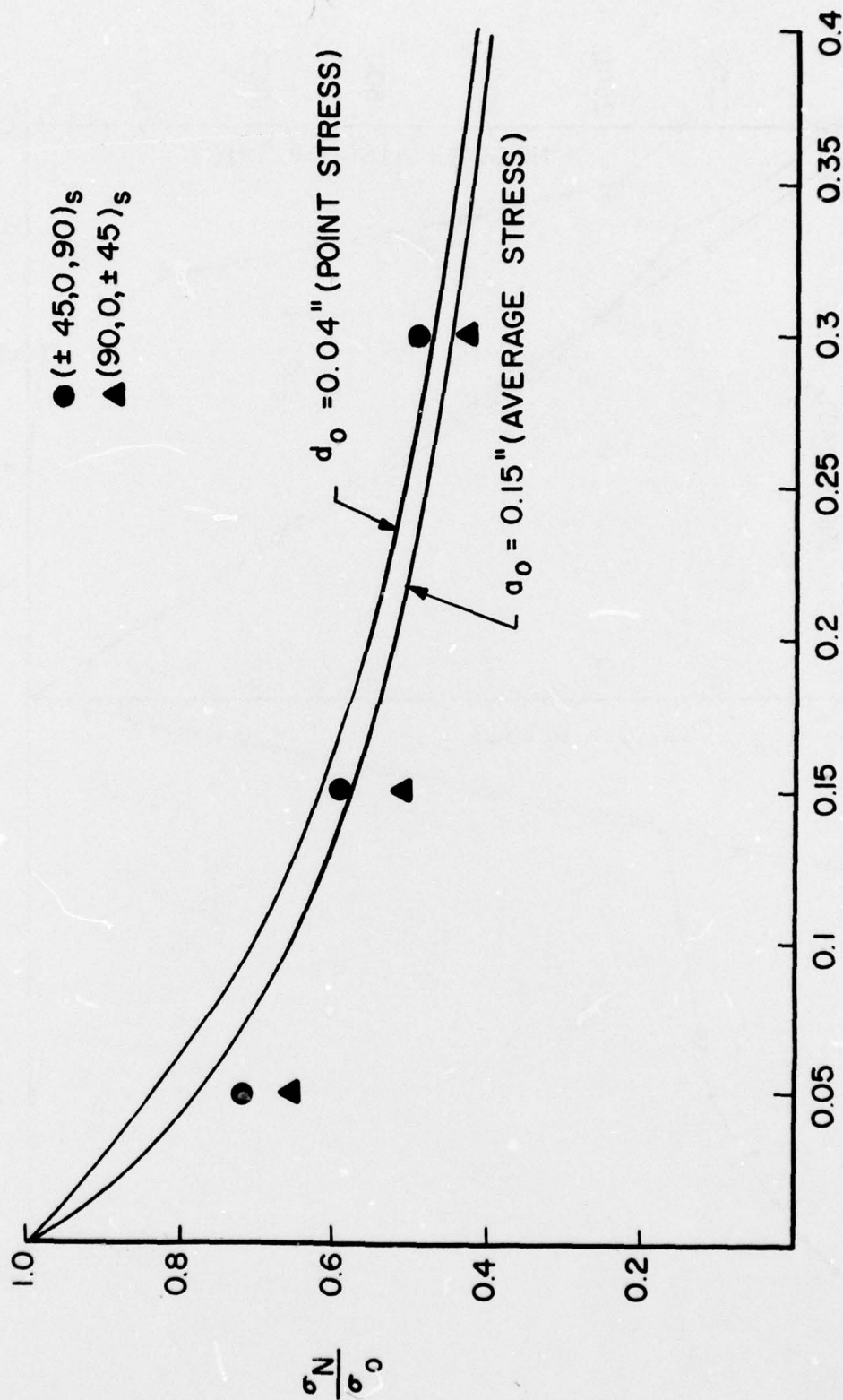


Figure 6. Comparison of predicted and experimental failure stresses for center cracks.



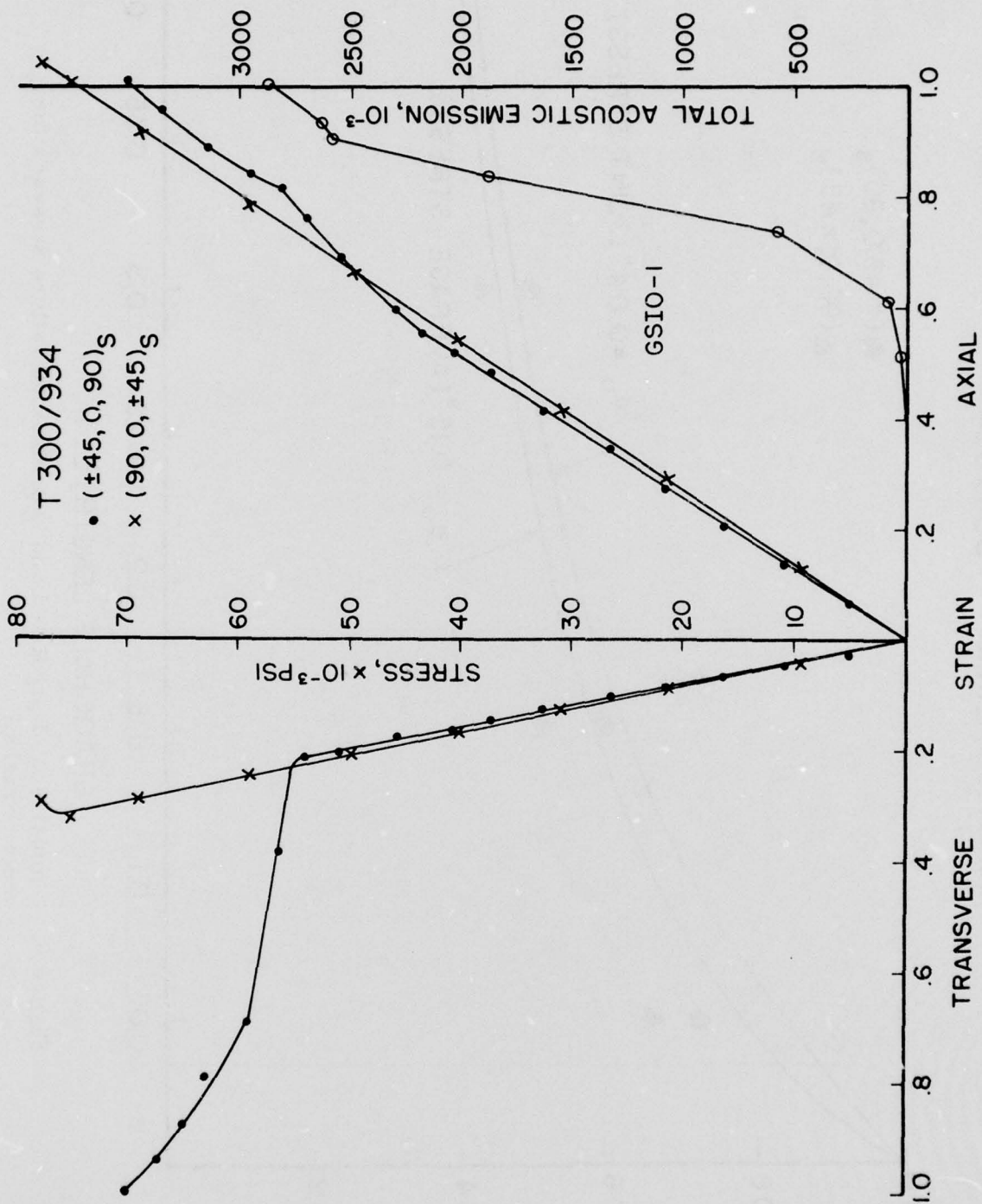


Figure 7. Typical longitudinal and axial stress-strain response of unnotched laminates.

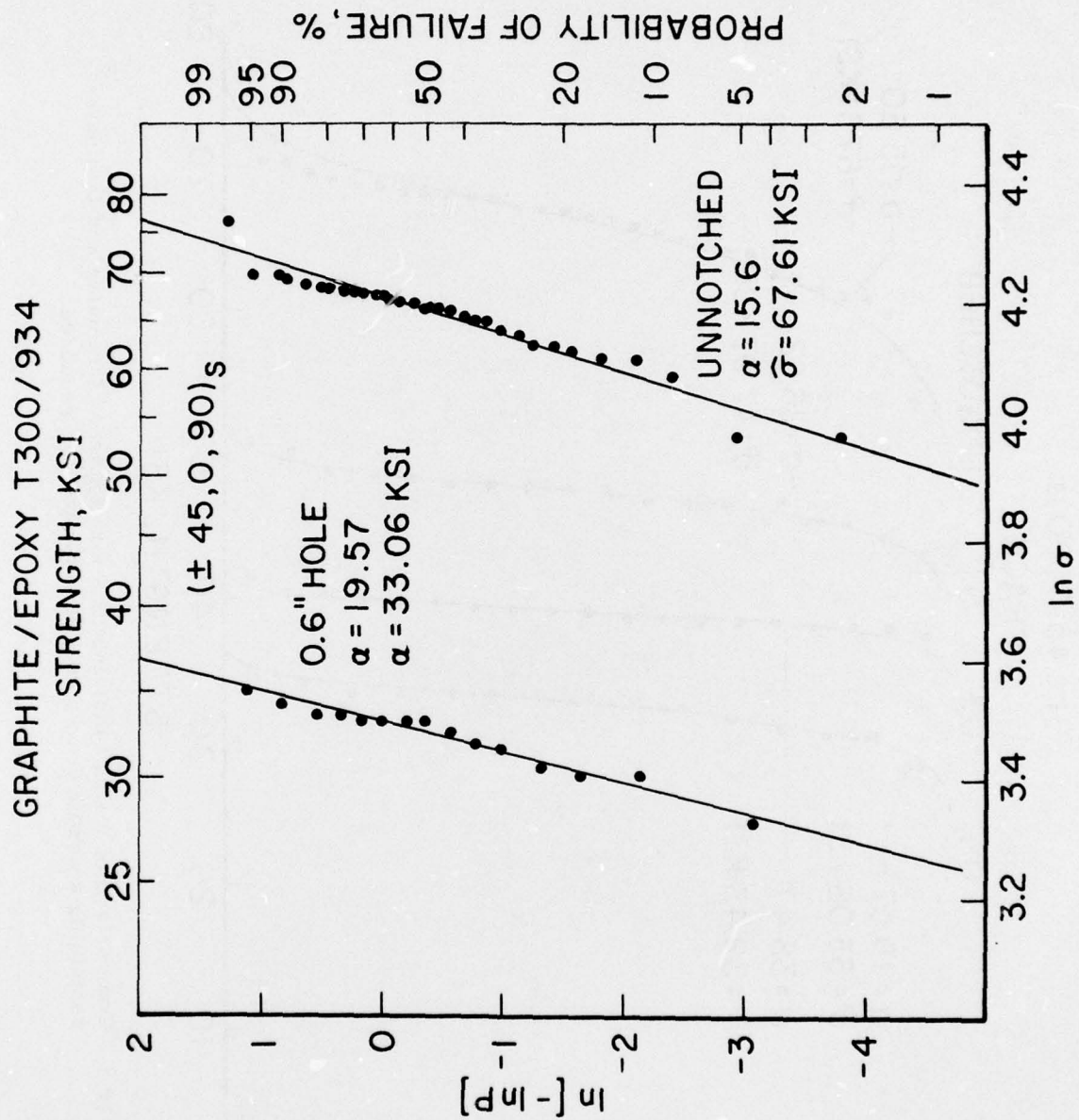


Figure 8. Typical data fit to linearized Weibull distribution.

GRAPHITE/EPOXY T300/934  
( $\pm 45, 0, 90$ )s

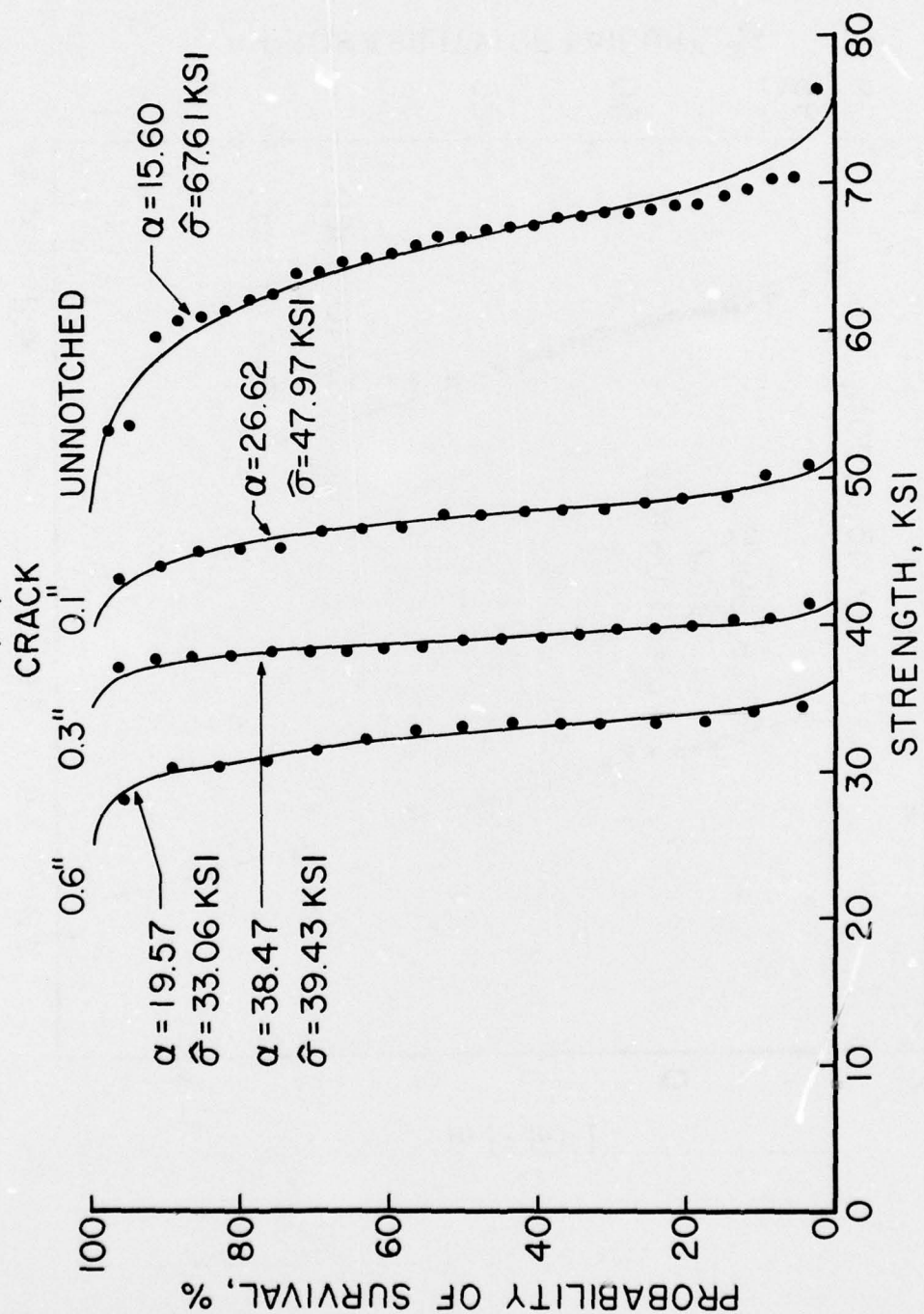


Figure 9. Comparison of Weibull distributions for unnotched laminates and laminates containing a center crack, ( $\pm 45, 0, 90$ )s stacking sequence.



GRAPHITE/EPOXY T300/934  
( $\pm 45, 0, 90$ )<sub>s</sub>

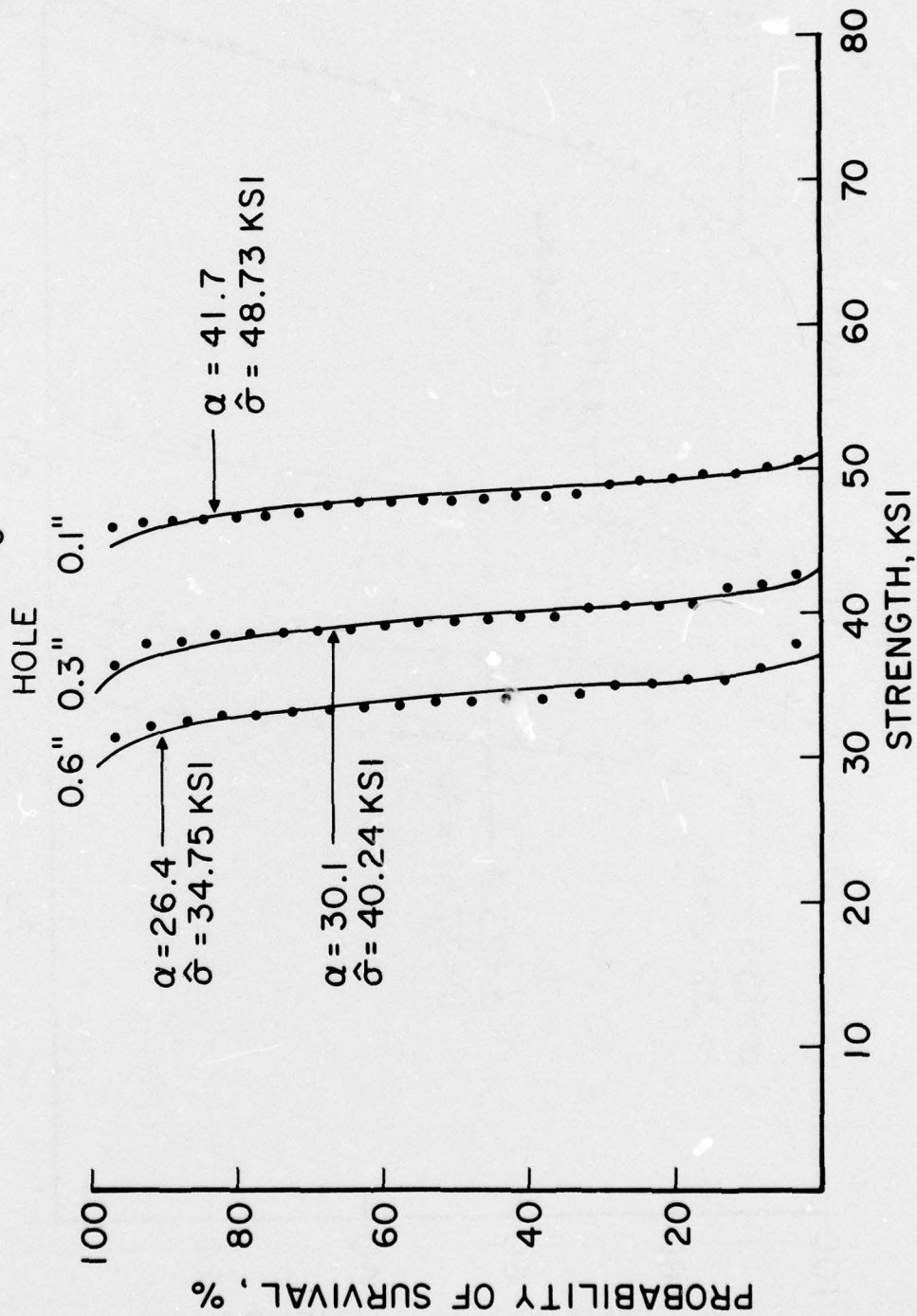


Figure 10. Comparison of Weibull distributions for laminates containing a circular hole, ( $\pm 45, 0, 90$ )<sub>s</sub> stacking sequence.

GRAPHITE / EPOXY T300 / 934  
(90, 0, ±45)<sub>s</sub>  
CRACK

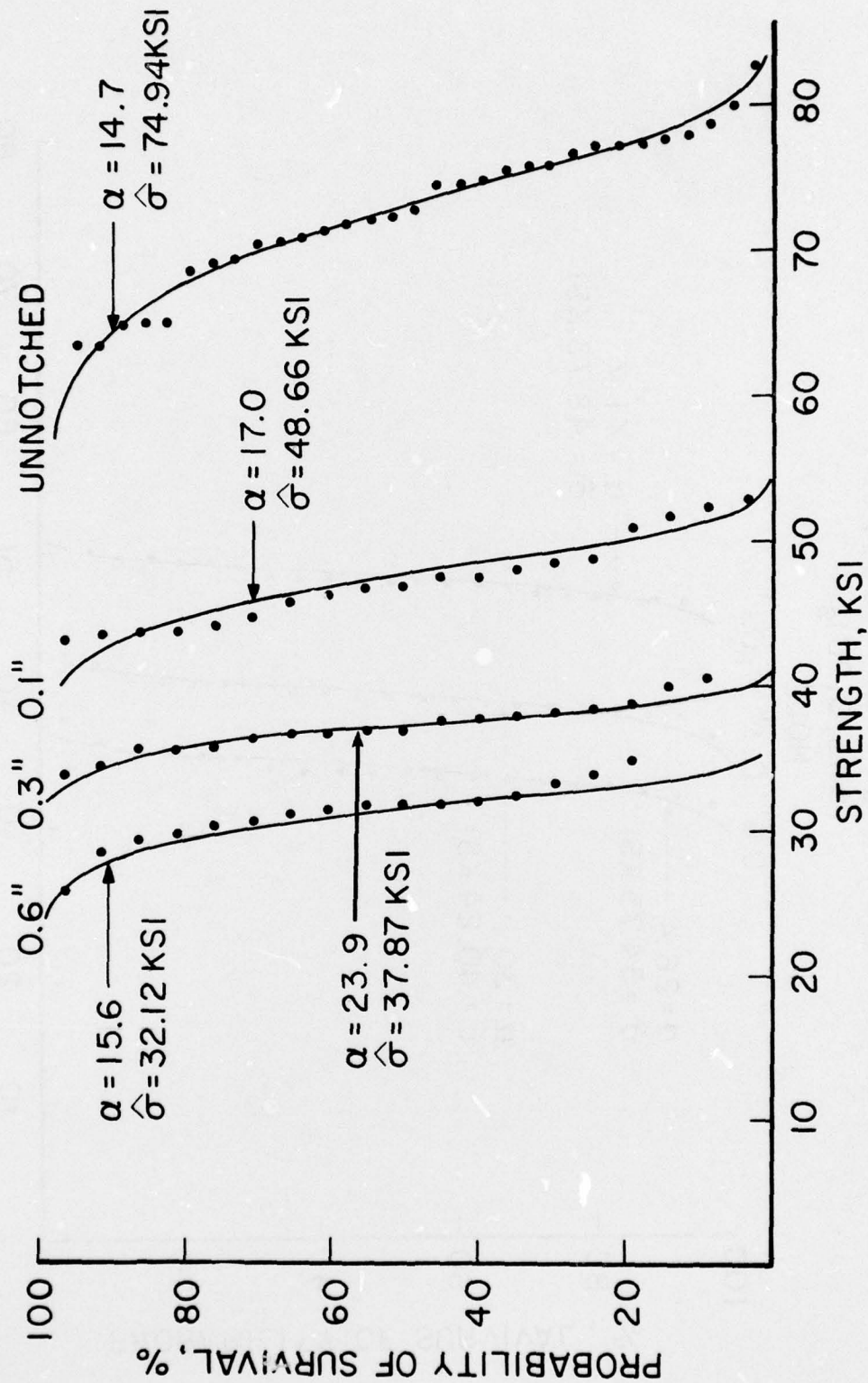


Figure 11. Comparison of Weibull distribution for unnotched laminates and laminates containing a center crack, (90, 0, ±45)<sub>s</sub> stacking sequence.

GRAPHITE/EPOXY T300/934  
(90,0,±45)<sub>s</sub>  
HOLE

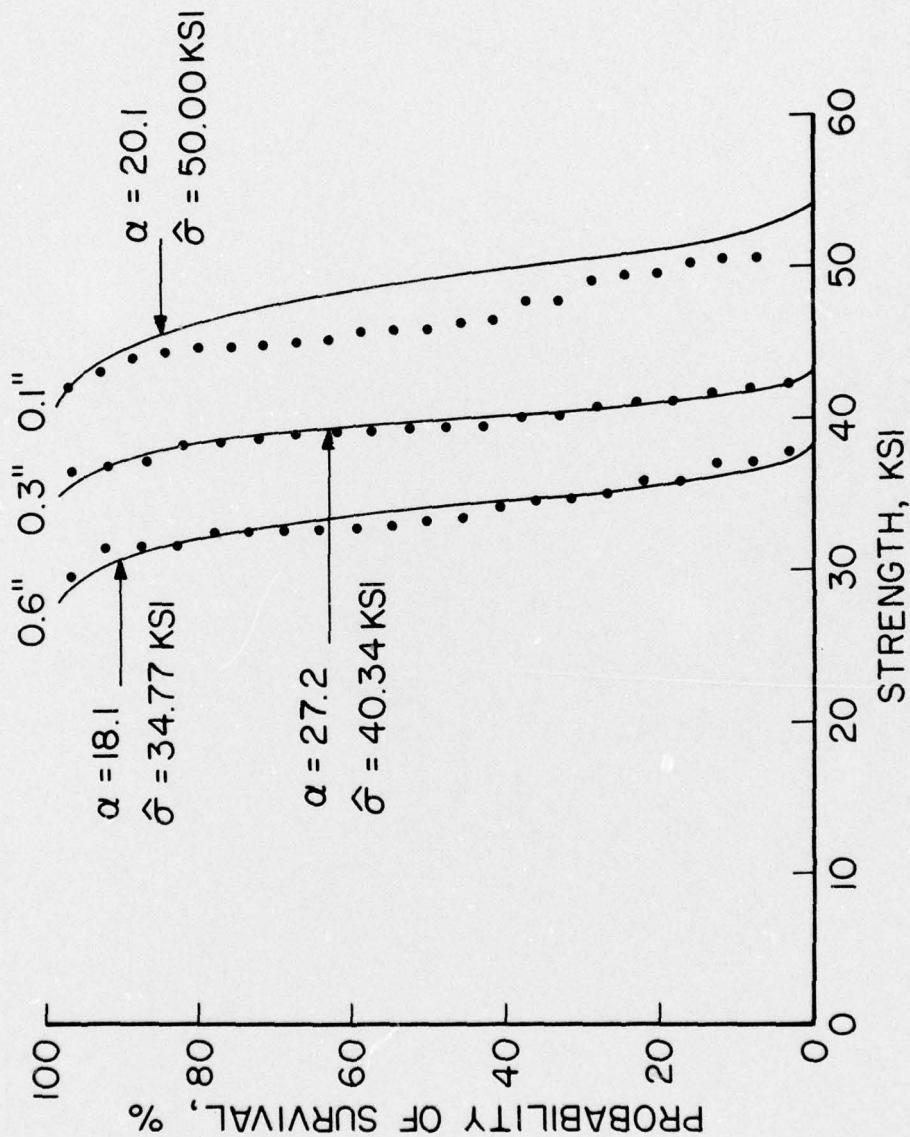


Figure 12. Comparison of Weibull distributions for laminates containing a circular hole, (90,0,±45)<sub>s</sub> stacking sequence.